Electronic Structure of Scandium and Titanium Carbide Cations, ScC^+ and TiC^+. Ground and Low-Lying States

Ioannis S. K. Kerkines and Aristides Mavridis*

Laboratory of Physical Chemistry, Department of Chemistry, National and Kapodistrian University of Athens, P.O. Box 64 004, 157 10 Zografou, Athens, Greece

Received: June 22, 2000

The monopositive scandium and titanium carbides, ScC^+ and TiC^+, have been studied by multireference methods coupled with quantitative basis sets. We have constructed potential energy curves for the ground and twelve low-lying excited states for both species, focusing on dissociation energies and bonding mechanisms. We have found that the ground states of ScC^+ and TiC^+ are of $^3\Pi$ and $^2\Sigma^+$ symmetries, with binding energies (D_0) of 68.8 (71.5) and 85.2 (86.7) kcal/mol at the MRCI (MRCI+Davidson correction) level of theory. These values are compared favorably with the corresponding experimental findings, $D_0(ScC^+) = 77.0 \pm 1.4$ and $D_0(TiC^+) = 93.4 \pm 5.5$ kcal/mol.

1. Introduction

Without doubt, the first-row transition metals play a central role in understanding the nature of the chemical bond. Given that, it is rather surprising that the literature, experimental or theoretical, on the diatomic carbides MC, M=Sc, Ti, ..., Cu, or on their positive ions is limited.[1] In particular, the available information on the cations MC^+ is scarce. Armentrout and co-workers[2] have measured the bond energies of ScC^+, TiC^+, and VC^+ using guided-ion-beam tandem mass spectrometry. Also, Hettich and Freiser[3] via Fourier transform mass spectrometry obtained the binding energies of FeC^+ and CoC^+ cations. However, the very nature of the mass spectrometric technique does not allow the determination of the system's state or other molecular parameters apart from the binding energy. On the theoretical side, Harrison[4] has published ab initio results on the CrC^+ system by employing MCSCF/CI methods, coupled with double-ζ+P quality basis sets. Table 1 summarizes the existing information on the first-row transition metal diatomic monopositive carbides.

With the purpose of obtaining reliable spectroscopic parameters, as well as to decipher the bonding mechanism on these "simple" systems, we have performed complete active space self-consistent field + singles + doubles configuration interaction (CASSCF+1+2 = MRCISD) calculations on ScC^+ and TiC^+ molecules; calculations are in progress for the rest of the series.

The first two excited states of Sc^+ cation, ^1D ($4s^13d^1$) and ^3F ($3d^2$), are 0.302 and 0.596 eV above the ground ^3D ($4s^13d^1$) state, respectively.[5] For the carbon atom, its first excited ^1D ($2s^22p^2$) state is located 1.260 eV above the ground ^3P ($2s^22p^2$) state.[5] The interaction $Sc^+(^3D, ^1D, ^3F) \otimes C(^3P)$ engenders in 72 $^{2S+1}|\Lambda|$ states, with S = 0, 1 or 2 and $|\Lambda| = 0, 1, 2, 3$, and 4 or $\Sigma^{\pm}$, Π, Δ, Φ, and Γ designation, respectively. Out of CASSCF calculations on all 72 states, 13 have been selected to be investigated at the MRCI level with the arbitrary criterion of being the lowest in energy at the CASSCF level of theory. Ten out of thirteen states correlate adiabatically to $Sc^+(^3D) + C(^3P)$ and three to $Sc^+(^3F) + C(^3P)$.

For the Ti^+ ion, the first two excited states, b^4F ($3d^3$) and ^2F ($4s^13d^2$), are 0.107 and 0.565 eV with respect to its ground a^4F ($4s^13d^2$) state.[5] Ninety-six states of $^{2S+1}|\Lambda|$ symmetry emanate out of the Ti^+ ($a\ ^4F, b^4F, ^2F$) $\otimes$ $C(^3P)$ interaction, with S = $^1/_2$, $^3/_2$, $^5/_2$, and $|\Lambda| = 0, 1, 2, 3$, and 4. Following the same selection procedure as in the ScC^+ case, 13 states have been picked and studied at the MRCI level of theory, all of them adiabatically correlating to the ground-state fragments $Ti^+(a^4F) + C(^3P)$.

TABLE 1: Existing Data on the MC^+ Molecules, M = Sc, Ti, V, Cr, Fe, and Co

species	method	D_0 (kcal/mol)	r_e (Å)
ScC^+	GIBTMS[a]	77.0 ± 1.4	
TiC^+	GIBTMS[a]	93.4 ± 5.5	
VC^+	GIBTMS[a,b]	91.1 ± 0.9	
CrC^+	ab initio[c]	31.5/X $^4\Sigma^-$[d]	1.735
		13.4/$^4\Pi$[d,e]	2.441
FeC^+	FTMS[f]	94 ± 7	
CoC^+	FTMS[f]	90 ± 7	

[a] Guided-ion-beam tandem mass spectrometry, ref 2a. [b] Reference 2b. [c] MCSCF−CI/DZ+P, ref 4. [d] Reference 4, $D_0 = D_e - \omega_e/2$. [e] It refers to D_e. [f] Fourier transform mass spectrometry, ref 3.

All in all for both molecules, the following 26 states have been studied. ScC^+: $^1\Sigma^+$(two), $^1\Pi$, $^1\Delta$, $^1\Gamma$, $^3\Sigma^-$(two), $^3\Pi$, $^3\Delta$-(two), $^3\Gamma$, $^5\Sigma^-$, $^5\Delta$, and TiC^+: $^2\Sigma^+$, $^2\Pi$(two), $^2\Delta$(two), $^2\Phi$, $^2\Gamma$, $^4\Pi$(two), $^4\Delta$, $^4\Phi$, $^6\Sigma^+$, $^6\Delta$.

At this point we could ask what the ground state is expected to be for the ScC^+ and TiC^+ species. In their (experimental) work Armentrout and co-workers[2a] suggest that the ground states of ScC^+ and TiC^+ should rather be singlets and doublets with "bond orders" of 2 and 2 $^1/_2$, respectively. Now, using simple valence-bond-Lewis (vbL) icons the following bonding scenarios can be envisaged for the ground ScC^+ case:

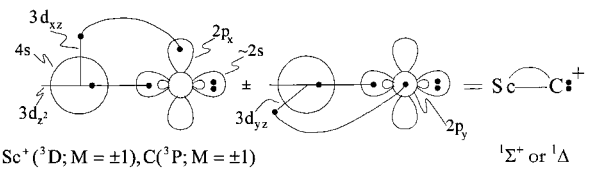

(I)

or

10.1021/jp002264d CCC: $19.00
Published on Web 11/23/2000

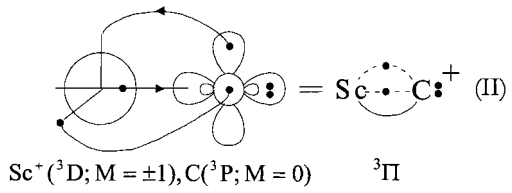

or

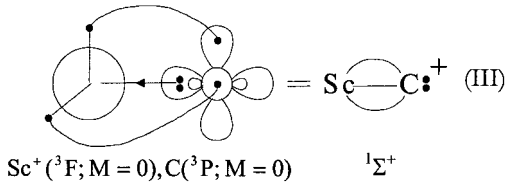

Scheme (I) predicts a ground state of $^1\Sigma^+$ ("+" sign) or $^1\Delta$ ("−" sign) symmetry with a σ and a π bond, scheme (II) a $^3\Pi$ state with 1 $^1/_2$ π bonds and $^1/_2$ σ bond, while scheme (III), in which the in situ Sc^+ atom finds itself in the excited ^3F state ($|^3F;M = 0\rangle = \sqrt{4/5}|d^1_{xz}d^1_{yz}\rangle + \sqrt{1/5}|d^1_{xy}d^1_{x^2-y^2}\rangle$), predicts a $^1\Sigma^+$ ground state with a triple bond. Scheme (I) conforms in essence with the predictions of Armentrout et al.[2a] However, our calculations predict that the ground state is the one suggested by scheme (II), i.e., of $^3\Pi$ symmetry, while the $^1\Sigma^+$(III), $^1\Delta$(I), and $^1\Sigma^+$(I) states are 14, 25, and 37 kcal/mol, respectively, above the $^3\Pi$ state (vide infra).

A similar analysis of TiC^+ implies that the ground state could be represented by either bonding schemes (IV) or (V):

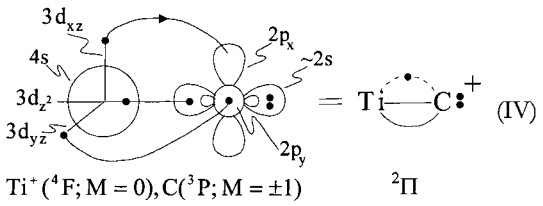

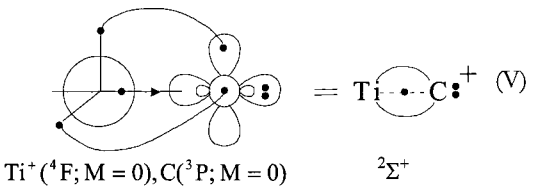

It turns out that the ground state is of $^2\Sigma^+$ symmetry, with the $^2\Pi$ being the first excited state ~15 kcal/mol above the X $^2\Sigma^+$ state (vide infra).

For almost all states studied in the present work, we report total energies, dissociation energies (D_e), bond distances (r_e), harmonic (ω_e) and anharmonic ($\omega_e x_e$) frequencies, Mulliken charges, and energy gaps (T_e), as well as potential energy curves (PEC). The construction of the latter is dictated by our desire for a better understanding of the bonding evolution along the reaction path.

2. Technical Details

For the Sc and Ti atoms, the ANO Gaussian basis sets 21s16p9d6f4g of Bauschlicher[6] were employed, but with the functions of g angular momentum removed. For the carbon atom, the correlation consistent basis set of quadruple-ζ quality, i.e., 12s6p3d2f1g of Dunning[7] was used. Both sets were generally contracted to [7s6p4d3f/5s4p3d2f1g], resulting in an electron basis set space of 121 spherical Gaussian functions (5d, 7f and 9g).

We have used the complete active space SCF + single + double replacements = MRCI methodology, which due to the relatively small number of active electrons (6 and 7 valence e^- in ScC^+ and TiC^+), is size consistent and, practically, size extensive. Indeed, our calculations show that for the ground states of ScC^+ and TiC^+ the size nonextensivity errors are 0.3 and 0.7 mhartree, respectively at the MRCI level.

The selected reference space for both molecules studied comprises of 10 orbital functions, correlating asymptotically to the "valence" occupied spaces of M^+ (4s+3d) and C (2s+2p) atoms. Considering the $1s^22s^22p^63s^23p^6$ and $1s^2$ electrons of Sc^+ or Ti^+ and C species, respectively, as core (inactive), our reference space is formed by distributing 6 or 7e^- among 10 orbitals. The reference spaces thus obtained range from 590 to 1746 configuration functions (CFs) in ScC^+ and from 522 to 3460 CFs in TiC^+, depending on the space-spin symmetry of the state studied. Note that although all of our calculations were done under C_{2v} symmetry restrictions, the CASSCF wave functions (but not the MRCI ones) display pure axial angular momentum symmetry, that is $|\Lambda| = 0$, 1, 2, 3, or 4. Dynamical (as opposed to quasidegenerate) correlation was obtained by single and double excitations out of the reference space, while core orbitals were always kept doubly occupied. To keep our computations within reasonable limits, the technique of internal contraction[8] MRCI was applied; as a result our largest CI expansion did not exceed the 800 000 CFs.

For purely technical reasons, we were also forced to use the state-average (SA)[9,10] approach. Energy losses due to the SA applied to these systems do not usually exceed 1 to 2 mhartree, with a synchronous bond length increase of 0.005 to 0.015 Å.[11] Basis set superposition error (BSSE) estimates, following the usual approach of Boys and Bernardi,[12] are 0.15 and 0.27 kcal/mol at the ground-state equilibrium geometries of ScC^+ and TiC^+, respectively, indicating the adequacy of our one-electron bases. Therefore, and for obvious reasons no BSSE corrections were applied to our reported results.

All of our calculations were performed with the MOLPRO 96.4 program.[13]

TABLE 2: Energies *E* (hartree) of the Ground ^3P State of the C Atom, and Atomic Energy Splittings ΔE (eV) in Different Methods (cc-pVQZ basis)

method	$-E$	ΔE ($^1D \leftarrow {}^3P$)	ΔE ($^1S \leftarrow {}^3P$)	ΔE ($^5S \leftarrow {}^3P$)
NHF[a]	37.688619			
sa-SCF[b]	37.688234			
SA-CASSCF[c]	37.705548	1.575	2.613	2.909
CISD	37.783239	1.299	2.734	4.109
MRCI	37.784932	1.287	2.695	4.109
MRCI+Q[d]	37.7879	1.27	2.70	4.18
expt[e]		1.260	2.680	4.179

[a] Numerical Hartree−Fock, ref 15. [b] Spherically averaged SCF. [c] State averaged CASSCF. [d] MRCI+multireference Davidson correction, ref 16. [e] Reference 5.

3. The Atoms

Total energies and resultant atomic energy splittings of Sc^+ and Ti^+ at the spherically averaged SCF and CISD level of theory are reported in refs 14 and 11, respectively. Table 2 reports total energies of the ground ^3P state of the C atom and also its ^5S, ^1S, $^1D \leftarrow {}^3P$ energy splittings at different levels of theory within the cc-pVQZ basis. Note the very good agreement between theory and experiment[5] of the atomic energy splittings

TABLE 3: Total Energies E (hartree), Dissociation Energies D_e (kcal/mol), Bond Lengths, r_e (Å), Harmonic ω_e and Anharmonic $\omega_e x_e$ Frequencies (cm^{-1}), and Energy Gaps T_e(kcal/mol) of Thirteen States of the ScC^+ Species at the MRCI[a](MRCI+Q)[b]Level of Theory

state[c]	$-E$	D_e[d]	r_e	ω_e	$\omega_e x_e$	T_e
X $^3\Pi(1)$	797.43944	69.8	1.908	709	4.0	0.0
	(0.4472)	(72.5)	(1.92)	(686)	(3.6)	
1 $^3\Sigma^-(1)$	797.42475	61.9	1.968	698	5.6	9.2
	(0.4344)	(65.4)	(1.99)	(596)	(3.5)	(8.1)
2 $^5\Delta(1)$	797.42199	59.0	2.102	654	4.1	11.0
	(0.4270)	(60.1)	(2.12)	(599)	(1.6)	(12.7)
3 $^1\Sigma^+(1)$	797.41706	58.0	1.809	767	9.5	14.0
	(0.4234)	(59.3)	(1.82)	(724)	(4.7)	(14.9)
4 $^5\Sigma^-(1)$	797.41590	55.1	2.061	673	4.6	14.8
	(0.4221)	(56.9)	(2.07)	(676)	(5.3)	(15.8)
5 $^3\Delta(1)$	797.41459	55.5	2.125	623	2.8	15.6
	(0.4207)	(56.8)	(2.13)	(609)	(2.9)	(16.6)
6 $^1\Pi(1)$	797.40966	51.1	1.891	711	0.9	18.7
	(0.4188)	(54.7)	(1.89)	(753)	(6.3)	(17.8)
7 $^1\Delta(1)$	797.39945	47.0	2.009	606	6.1	25.1
	(0.4080)	(49.6)	(2.02)	(591)	(4.7)	(24.6)
8 $^3\Sigma^-(2)$	797.39653	44.6	2.107	616	5.2	26.9
	(0.4033)	(46.1)	(2.09)	(605)	(6.8)	(27.6)
9 $^1\Sigma^+(2)$	797.38011		2.002	652	6.7	37.2
	(0.3873)		(2.00)	(663)	(7.7)	(37.6)
10 $^3\Gamma(1)$	797.36895		2.129			44.2
	(0.3765)		(2.14)			(44.4)
11 $^1\Gamma(1)$	797.36788	42.3	2.139	597	3.3	44.9
	(0.3747)	(44.2)	(2.15)	(590)	(3.4)	(45.5)
12 $^3\Delta(2)$	797.36618	23.8	2.099			46.0
	(0.3728)	(25.8)	(2.11)			(46.7)

[a] Internally contracted MRCI. [b] "+Q" refers to the multireference Davidson correction, ref 16. [c] Numbers in parentheses after the term symbol indicate the energy ordering, but within the same symmetry manifold. [d] D_e with respect to the adiabatic products.

ensuring the adequacy of the carbon basis set. Corresponding agreement between theory[14,11] and experiment[5] for the Sc^+ and Ti^+ atoms can be deemed as satisfactory, at least for the splittings ^3F, $^1D \leftarrow {}^3D$ of Sc^+ and $b^4F \leftarrow a^4F$, $a^2F \leftarrow b^4F$ of Ti^+.

4. Results and Discussion

In section 4.1 we discuss the ScC^+ and in 4.2 the TiC^+ molecule. With the exception of the ground states marked X, in all other states a number in front of the molecular term symbol indicates the absolute energy ordering of the state with respect to the X state; a second number into parenthesis gives the ordering of the states within the same symmetry manifold.

4.1. The ScC^+ Molecule. Table 3 lists the pertinent numerical results of all 13 computed states of the ScC^+ cation, whereas Table 4 gives the adiabatic asymptotic descriptions $|Sc^+>|C>$, leading CASSCF equilibrium configurations, and CASSCF Mulliken atomic populations. Figure 1 depicts MRCI potential energy curves.

X $^3\Pi(1)$, 6 $^1\Pi(1)$. At about 5 bohr, the X $^3\Pi$ state suffers an avoided crossing with another $^3\Pi$ state, resulting at the equilibrium in a $M = \pm 1, 0$ combination. The leading configuration and the Mulliken distributions (Table 4), indicate that the two atoms are held together by $1^1/_2$ π bonds and a half σ bond; along the π frame, $\sim$0.2 e^- are transferred from C to Sc^+, while $\sim$0.5 e^- are moving in the opposite direction through the σ frame. The bonding is captured nicely by the valence bond Lewis (vbL) icon, scheme (II) of the introduction. At the MRCI (MRCI+Q) level, a $D_0 = D_e - \omega_e/2 = 68.8$ (71.5) kcal/mol is predicted, in acceptable agreement with the experimental value[2a], $D_0 = 77.0 \pm 1.4$ kcal/mol (see Table 1).

We can think of the 6 $^1\Pi(1)$ state as arising from the X state by a spin flip and (adiabatically) correlating to the same atomic fragments as the X $^3\Pi$ state. At about 4.2 bohr, an avoided crossing occurs with another (not calculated) $^1\Pi$ state, resulting as in the X $^3\Pi$ state to an M change: $M = (\pm 2, \mp 1) \rightarrow (\pm 1, 0)$. As revealed from Table 4 the binding process is similar to the X $^3\Pi$ state and can be adequately described by scheme (II). Both states have practically the same internuclear distance; the 19 kcal/mol destabilization of the 6 $^1\Pi$ state as compared to the X state is due to the spin flip in the former.

1 $^3\Sigma^-(1)$, 4 $^5\Sigma^-(1)$, 8 $^3\Sigma^-(2)$. The first excited state, 1 $^3\Sigma^-$, lies 9.2 kcal/mol above the X state. The leading equilibrium CASSCF CFs in conjunction with the equilibrium Mulliken distributions (Table 4), and the corresponding populations at infinity, r_∞ ($4_s^{1.0}\ 3d_{xz}^{0.50}\ 3d_{yz}^{0.50}/2s^{1.96}\ 2p_z^{1.0}\ 2p_x^{0.52}\ 2p_y^{0.52}$) suggest that the bonding is comprised of two-half π bonds and a σ bond. Through the π frame about 0.4 e^- are transferred from the metal to the carbon atom, while via the σ skeleton 0.2 e^- are returning to the hybrid $(4s3d_{z^2})^{1.20}$ orbital on the metal. Overall the in situ C atom carries a charge of 0.25 e^-. A vbL picture describing the bonding can be drawn as follows

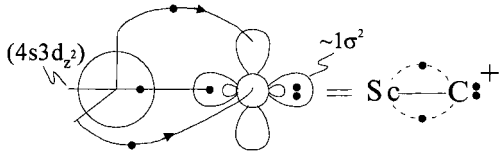

At the MRCI level, a $D_e = 61.9$ kcal/mol is obtained at $r_e = 1.968$ Å, Table 3.

By breaking the σ bond of the 1 $^3\Sigma^-$ state, the 4 $^5\Sigma^-$ state is obtained. From the two configuration description and the Mulliken CASSCF populations, two-half π bonds can be clearly discerned with 0.60 e^- migrating from Sc^+ to C via the π frame. Along the σ frame about 0.4 e^- are transferred from C to Sc^+, resulting in a half σ "interaction". Pictorially, the following vbL scheme can be adopted

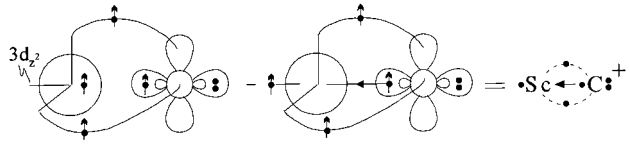

At the MRCI level, a $D_e = 55.1$ kcal/mol is calculated with respect to the ground-state products, at $r_e = 2.061$ Å, 0.10 Å longer than the bond length of the 1 $^3\Sigma^-$ state.

At 17.7 kcal/mol above the 1 $^3\Sigma^-$ the 8 $^3\Sigma^-$ state is located; Table 4 gives its lineage and main CASSCF configurational description. The bonding comprises two-half π bonds and a "dative" σ bond originating from the Sc^+ cation, resulting in $D_e = 44.6$ kcal/mol at $r_e = 2.107$ Å, Table 3.

2 $^5\Delta(1)$, 5 $^3\Delta(1)$, 12 $^3\Delta(2)$. The 2 $^5\Delta$ state is well represented by its Hartree−Fock description, Table 4. The populations at infinity (r_∞) $4s^{1.0}\ 3d_{xy}^{1.0}/2s^{1.96}\ 2p_z^{0.04}\ 2p_x^{1.0}\ 2p_y^{1.0}$ and at r_e, in conjunction with the single configurational description dictate the following bonding picture:

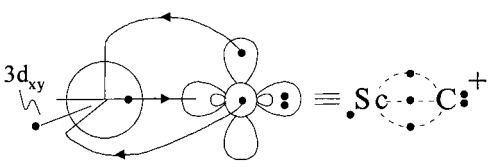

Three half bonds, two π and one σ, hold the two atoms together,

TABLE 4: Asymptotic Fragments, Leading Equilibrium CASSCF CFs, and Equilibrium CASSCF Mulliken Atomic Populations of the 13 ScC^+ States Studied

state	adiabatic fragments[a]	dominant equilibrium CASSCF CFs	equilibrium CASSCF Mulliken atomic populations										
			Sc							C			
			4s	$4p_\sigma$	$4p_\pi$	$3d_\sigma$	$3d_{xz}$	$3d_{yz}$	$3d_\delta$	2s	$2p_z$	$2p_x$	$2p_y$
$X\ ^3\Pi(1)$	$\|\pm 2\rangle\|\mp 1\rangle$	$0.89\|1\sigma^2 2\sigma^1 1\pi_x^1 1\pi_y^2\rangle$[c]	0.10	0.05	0.10	0.36	0.31	0.79		1.73	0.76	0.66	1.10
$1\ ^3\Sigma^-(1)$	$\|\pm 1\rangle\|\mp 1\rangle$	$0.61\|1\sigma^2 2\sigma^1 \overline{3\sigma}^1 1\pi_x^1 1\pi_y^1\rangle + 0.59\|1\sigma^2 2\sigma^2 1\pi_x^1 1\pi_y^1\rangle$	0.32	0.03	0.04	0.87	0.26	0.26		1.79	0.97	0.72	0.72
$2\ ^5\Delta(1)$	$\|\pm 2\rangle\|0\rangle$	$0.98\|1\sigma^2 2\sigma^1 1\pi_x^1 1\pi_y^1 1\delta_-^1\rangle$[d]	0.14	0.05	0.06	0.18	0.13	0.13	1.0	1.78	0.83	0.83	0.83
$3\ ^1\Sigma^+(1)$	$\|\pm 1\rangle\|\mp 1\rangle$	$0.89\|1\sigma^2 1\pi_x^2 1\pi_y^2\rangle$	0.06	0.02	0.06	0.13	0.73	0.73	0.02	1.78	0.10	1.15	1.15
$4\ ^5\Sigma^-(1)$	$\|\pm 1\rangle\|\mp 1\rangle$	$0.81\|1\sigma^2 2\sigma^1 4\sigma^1 1\pi_x^1 1\pi_y^1\rangle - 0.54\|1\sigma^2 2\sigma^1 3\sigma^1 1\pi_x^1 1\pi_y^1\rangle$	0.61	0.04	0.08	0.75	0.14	0.14		1.78	0.80	0.82	0.82
$5\ ^3\Delta(1)$	$\|\pm 1\rangle\|\pm 1\rangle$	$0.95\|1\sigma^2 2\sigma^1 1\pi_x^1 1\pi_y^1 \overline{1\delta}_-^1\rangle$[d]	0.15	0.04	0.02	0.22	0.14	0.14	0.99	1.75	0.85	0.84	0.84
$6\ ^1\Pi(1)$	$\|\pm 2\rangle\|\mp 1\rangle$	$0.84\|1\sigma^2 2\sigma^1 \overline{1\pi}_x^1 1\pi_y^2\rangle$[c]	0.10	0.04	0.09	0.41	0.41	0.71	0.02	1.78	0.67	0.56	1.17
$7\ ^1\Delta(1)$	$\|\pm 1\rangle\|\pm 1\rangle$	$0.57(\|1\sigma^2 2\sigma^2 1\pi_x^2\rangle - \|1\sigma^2 2\sigma^2 1\pi_y^2\rangle)$[d] $0.81\|1\sigma^2 2\sigma^2 1\pi_x^1 \overline{1\pi}_y^1\rangle$[e]	0.10	0.02	0.06	0.71	0.40	0.40	0.05	1.90	1.18	0.57	0.57
$8\ ^3\Sigma^-(2)$	$\|0\rangle\|0\rangle$	$0.76\|1\sigma^2 2\sigma^2 1\pi_x^1 1\pi_y^1\rangle$	0.44	0.03	0.04	0.31	0.47	0.47	0.04	1.91	1.24	0.52	0.52
$9\ ^1\Sigma^+(2)$	$\|\pm 1\rangle\|\mp 1\rangle$[b]	$0.46(\|1\sigma^2 2\sigma^2 1\pi_x^2\rangle + \|1\sigma^2 2\sigma^2 1\pi_y^2\rangle)$	0.08	0.02	0.06	0.63	0.38	0.38	0.25	1.85	1.05	0.64	0.64
$10\ ^3\Gamma(1)$	$\|\pm 3\rangle\|\pm 1\rangle$[b]	$-0.58\|1\sigma^2 2\sigma^1 1\pi_x^1 \overline{1\pi}_y^1 1\delta_-^1\rangle + 0.34\|1\sigma^2 2\sigma^1 \overline{1\pi}_x^1 1\pi_y^1 1\delta_-^1\rangle$ $+0.47(\|1\sigma^2 2\sigma^1 1\pi_y^2 1\delta_+^1\rangle - \|1\sigma^2 2\sigma^1 1\pi_x^2 1\delta_+^1\rangle)$[d]	0.09	0.03	0.04	0.17	0.25	0.25	1.0	1.85	0.85	0.73	0.73
$11\ ^1\Gamma(1)$	$\|\pm 3\rangle\|\pm 1\rangle$[b]	$0.58\|1\sigma^2 2\sigma^1 1\pi_x^1 \overline{1\pi}_y^1 \overline{1\delta}_-^1\rangle$ $-0.47(\|1\sigma^2 2\sigma^1 1\pi_y^2 \overline{1\delta}_+^1\rangle - \|1\sigma^2 2\sigma^1 1\pi_x^2 \overline{1\delta}_+^1\rangle)$[d]	0.09	0.03	0.04	0.14	0.27	0.27	1.0	1.84	0.88	0.70	0.70
$12\ ^3\Delta(2)$	$\|\pm 2\rangle\|0\rangle$	$0.60(\|1\sigma^2 2\sigma^1 3\sigma^1 1\pi_x^2\rangle - \|1\sigma^2 2\sigma^1 3\sigma^1 1\pi_y^2\rangle)$[d]	0.68	0.04	0.04	0.45	0.34	0.34	0.12	1.84	0.85	0.65	0.65

[a] $|Sc^+;\ ^3D;\ M\rangle|C;\ ^3P;\ M\rangle$. [b] $|Sc^+;\ ^3F;\ M\rangle|C;\ ^3P;\ M\rangle$. [c] B_1 symmetry component. [d] A_1 symmetry component. [e] A_2 symmetry component.

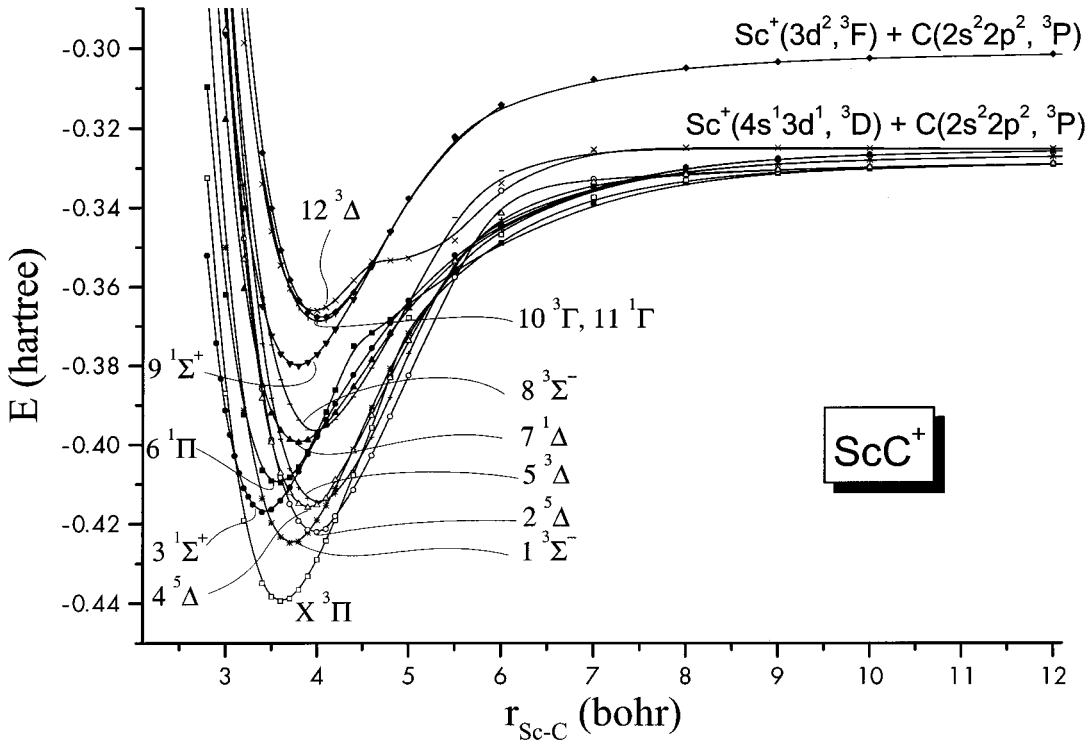

Figure 1. Potential energy curves of the ScC^+ system. MRCI level of theory.

giving rise to a $D_e = 59.0$ kcal/mol and $r_e = 2.102$ Å at the MRCI level. Note that the $3d_{xy}$ (or $3d_{x^2-y^2}$) electron is strictly localized on Sc^+ with no participation in the bonding process. Through the π system $\sim$0.3 e^- are diffused toward the metal creating the two-half π bonds, whereas via the σ system $\sim$0.6 e^- are returning to the C atom, essentially filling the empty $2p_z$ function; overall 0.30 e^- are moving from Sc^+ to the C atom.

Apart from a spin flip of the δ_- (or δ_+) observer electron, the $5\ ^3\Delta(1)$ state is very similar to the previously discussed $2\ ^5\Delta$ state, as is evidenced from the leading HF configuration, Table 4. As a result, the binding mechanism, D_e, r_e, and ω_e are practically the same as those of the $2\ ^5\Delta$ state, Table 3. However, it should be mentioned that its PEC suffers an avoided crossing around 5.5 bohr with the incoming $12\ ^3\Delta$ state, resulting in an

M change, so diabatically it correlates to $Sc^+(^3D; M = \pm 2) + C(^3P; M = 0)$.

As we approach the equilibrium of the 12 $^3\Delta(2)$ state, two avoided crossings occur: one, previously mentioned around 5.5 bohr with the 5 $^3\Delta(1)$ state, and a second one at about 4.7 bohr with a third (not calculated) $^3\Delta$ state correlating to Sc^+ (^1D; M $= \pm 1$) + C(^3P; M $= \pm 1$). In the π frame, 0.3 e^- are shifted from Sc^+ to C with approximately the same amount of charge returning to Sc^+ from C through the σ skeleton. Out of the 13 states studied, this is the only one in which no charge transfer is observed from Sc^+ to C, the atoms remaining in their asymptotic charge mode. Within the A_1 symmetry component we can draw the following bonding icon

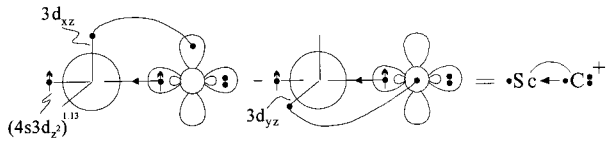

The single π bond is reflected in the rather weak binding of 23.8 kcal/mol at $r_e = 2.099$ Å, Table 3. It is worthwhile to recall the role of symmetry in the descriptive phenomenology of bonding: In the A_2 component, the corresponding bonding picture will be

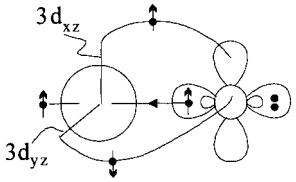

indicating two-half π bonds.

3 $^1\Sigma^+(1)$, 9 $^1\Sigma^+(2)$. Table 4 lists the dominant equilibrium configurations and asymptotic wave functions. A third, not calculated at the MRCI level $^1\Sigma^+(3)$ state, correlates to $Sc^+(^3F; M = 0)$+C(^3P; M $= 0$). An avoided crossing around 4.5 bohr between the $3^1\Sigma^+(1)$ and $^1\Sigma^+(3)$ states, transfers the character of the latter to the equilibrium of the former, so the $3^1\Sigma^+$ state correlates diabatically to $Sc^+(^3F; M = 0)$+C(^3P; M $= 0$).

In the $3^1\Sigma^+$ state we have the formation of two π bonds with the synchronous migration of $\sim$0.3 e^- from Sc^+ to the C atom via the π system, and a transfer of $\sim$0.2 e^- through the σ system from C to Sc^+ resulting to a "dative" σ bond. The consolidation of a pure triple bond is succinctly shown in scheme (III) of the introduction. As expected, the bond length of this state ($r_e =$ 1.809 Å, Table 3), is the shortest of all states studied, shorter by 0.10 Å from the ground X $^3\Pi$ state. With respect to the ground-state atoms, a $D_e = 58.0$ kcal/mol is obtained; however, the *internal bond strength*, i.e., with respect to $Sc^+(^3F)$ + C(^3P), is $\sim$74 kcal/mol.

The bonding situation is rather unclear in the 9 $^1\Sigma^+(2)$ state due to the multitude of CFs contributing significantly to the CASSCF wave function. From the dominant CFs, the Mulliken populations at r_e (Table 4) and the populations at r_∞ ($3d_{z^2}^{0.40}$ $3d_{xz}^{0.50}$ $3d_{yz}^{0.50}$ $3d_{x^2-y^2}^{0.30}$ $3d_{xy}^{0.30}$/$2s^{1.96}$ $2p_z^{1.0}$ $2p_x^{0.52}$ $2p_y^{0.52}$), one can claim that the two atoms are held together by a π and a σ bond. The π and σ frames carry $2 \times (0.64 + 0.38) = 2.04$, and $0.63 + 0.08 + 0.02 + 1.05 = 1.78$ e^- respectively, without counting the 2s electrons on the C atom. A total transfer of 0.20 e^- is observed from Sc^+ to C. The bonding icon is that of scheme (I) of the introduction with the "+" sign. Due to technical reasons, we were unable to compute the MRCI PEC beyond 6 bohr, Figure 1. At the MRCI level, we estimate a $D_e = 50$ kcal/mol with respect to $Sc^+(^3F)$ + C(^3P) and $r_e = 2.002$ Å.

TABLE 5: Total Energies *E* (hartree), Dissociation Energies D_e (kcal/mol), Bond Lengths, r_e (Å), Harmonic ω_e and Anharmonic $\omega_e x_e$ Frequencies (cm^{-1}), and Energy Gaps T_e (kcal/mol) of Thirteen States of the TiC^+ Species at the MRCI[a](MRCI+Q)[b]Level of Theory

state[c]	$-E$	D_e[d]	r_e	ω_e	$\omega_e x_e$	T_e
X $^2\Sigma^+(1)$	886.13945	86.4	1.696	859	2.7	0.0
	(0.1455)	(88.0)	(1.70)	(847)	(4.9)	
1 $^2\Pi(1)$	886.11613	71.5	1.764	734	8.3	14.6
	(0.1222)	(72.7)	(1.77)	(723)	(9.0)	(14.6)
2 $^4\Pi(1)$	886.11131	68.5	1.853	731	4.3	17.7
	(0.1181)	(70.2)	(1.86)	(722)	(5.3)	(17.2)
3 $^4\Phi(1)$	886.11102	68.4	1.864	702	4.0	17.8
	(0.1177)	(70.0)	(1.87)	(690)	(4.8)	(17.4)
4 $^2\Phi(1)$	886.10498	64.9	1.899	678	3.9	21.6
	(0.1112)	(66.3)	(1.90)	(671)	(3.6)	(21.5)
5 $^4\Delta(1)$	886.10022	61.8	1.911	714	7.2	24.6
	(0.1074)	(63.7)	(1.92)	(707)	(4.4)	(23.9)
6 $^2\Delta(1)$	886.09246	56.9	1.945			29.5
	(0.0992)	(58.6)	(1.95)			(29.1)
7 $^2\Pi(2)$	886.08656	53.5	1.860	776	6.5	33.2
	(0.0930)	(55.0)	(1.86)	(761)	(6.7)	(32.9)
8 $^6\Delta(1)$	886.08495	52.2	2.033	635	6.5	34.2
	(0.0927)	(54.5)	(2.04)	(628)	(8.4)	(33.1)
9 $^6\Sigma^+(1)$	886.07888	48.7	2.032	649	4.4	38.0
	(0.0877)	(51.6)	(2.04)	(634)	(4.9)	(36.3)
10 $^2\Delta(2)$	886.07697	47.5	1.803			39.2
	(0.0833)	(48.9)	(1.81)			(39.0)
11 $^2\Gamma(1)$	886.07592	46.9	1.960			39.9
	(0.0827)	(48.2)	(1.97)			(39.4)
12 $^4\Pi(2)$	886.07076	43.7	1.875	693	4.4	43.1
	(0.0781)	(45.7)	(1.88)	(684)	(7.2)	(42.3)

[a] Internally contracted MRCI. [b] "+Q" refers to the multireference Davidson correction, ref 16. [c] Numbers into parentheses after the term symbol indicate the ordering according to energy but within the same symmetry manifold. [d] D_e with respect to the adiabatic products.

7 $^1\Delta(1)$. This state is similar to the 9 $^1\Sigma^+$ state described above. Table 4 gives the dominant CASSCF CFs in both A_1 and A_2 symmetries. The bonding is described pictorially either by Scheme 1 ("−" sign) of the introduction (A_1 component) or by the following vbL icon (A_2 component):

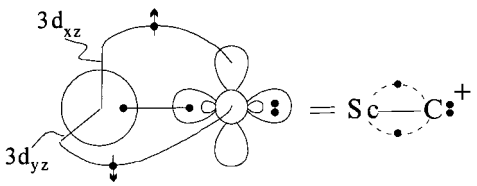

Clearly, the two bonding descriptions are equivalent (see also the 12 $^3\Delta$ state), implying a σ and a π bond (A_1 component, scheme (I)), or a σ and two equivalent half π bonds coupled into a singlet (A_2 component). From Table 3 we read that the MRCI D_e and r_e values are 47.0 kcal/mol, and 2.009 Å, respectively. As expected, both these values are very close to those of the 9 $^1\Sigma^+$ state (vide supra).

10 $^3\Gamma(1)$, 11 $^1\Gamma(1)$. By a spin flip of, for instance, the $\delta_\pm$ electron ($\delta_\pm^1 \rightarrow \bar{\delta}_\pm^1$) of the $^3\Gamma$, the $^1\Gamma$ state is obtained. These two states are degenerate within the accuracy of our methods, differing by 0.7 (1.1) kcal/mol at the MRCI (MRCI+Q) level. At $r_e = 2.139$ Å, a $D_e = 42.3$ kcal/mol is predicted for the $^1\Gamma$ state with respect to $Sc^+(^3F)$ + C(^3P). In both states about 0.2 e^- are transferred from Sc^+ to C. Finally, it should be stated that technical reasons allowed for only a part of the $^3\Gamma$ state PEC to be completed.

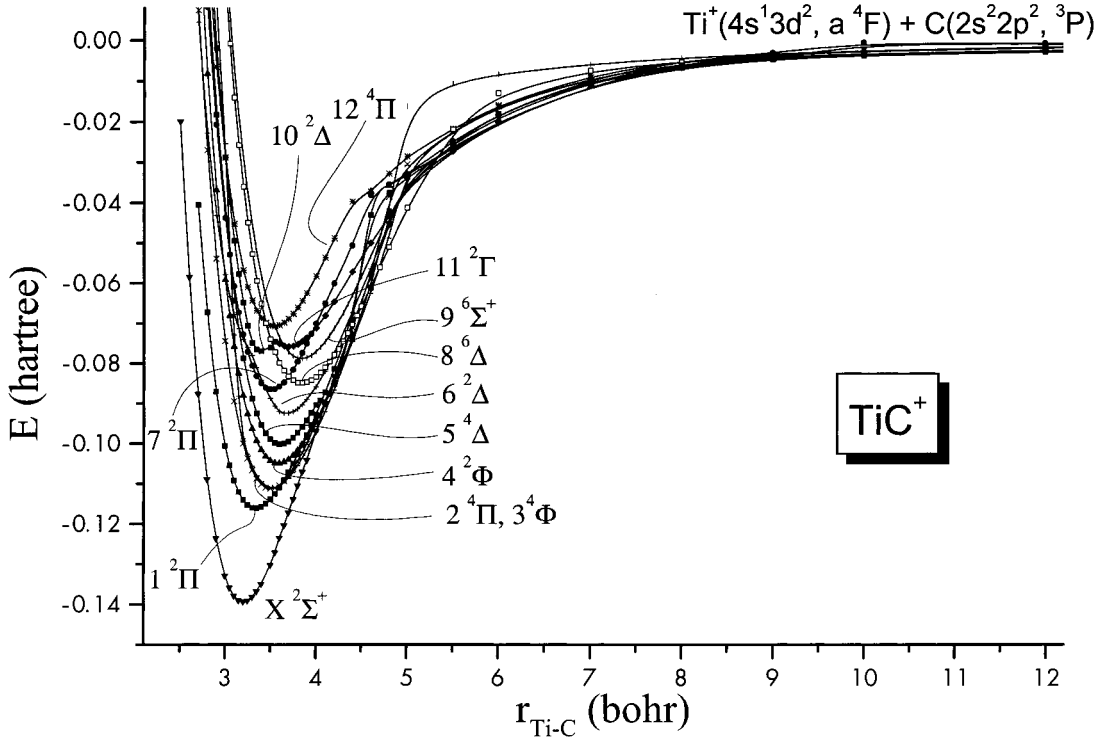

Figure 2. Potential energy curves of the TiC^+ system. MRCI level of theory.

TABLE 6: Asymptotic Fragments, Leading Equilibrium CASSCF CFs, and Equilibrium CASSCF Mulliken Atomic Populations of the 13 TiC^+ States Studied

state	adiabatic fragments[a]	dominant equilibrium CASSCF CFs	equilibrium CASSCF Mulliken atomic populations										
			Ti							C			
			4s	$4p_\sigma$	$4p_\pi$	$3d_\sigma$	$3d_{xz}$	$3d_{yz}$	$3d_\delta$	2s	$2p_z$	$2p_x$	$2p_y$
$X\ ^2\Sigma^+(1)$	$\|\pm1\rangle\|\mp1\rangle$	$0.87\|1\sigma^2 2\sigma^1 1\pi_x^2 1\pi_y^2\rangle$	0.08	0.06	0.06	0.61	0.98	0.98	0.04	1.74	0.54	0.94	0.94
$1\ ^2\Pi(1)$	$\|\pm1\rangle\|0\rangle$	$0.81\|1\sigma^2 2\sigma^2 1\pi_x^1 1\pi_y^2\rangle$[b]	0.09	0.08	0.05	1.0	0.47	0.96	0.14	1.82	0.87	0.57	0.91
$2\ ^4\Pi(1)$	$\|\pm2\rangle\|\mp1\rangle$	$0.62(\|1\sigma^2 2\sigma^1 1\pi_x^2 1\pi_y^1 1\delta_-^1\rangle + \|1\sigma^2 2\sigma^1 1\pi_x^1 1\pi_y^2 1\delta_+^1\rangle)$[b]	0.13	0.03	0.04	0.42	0.62	0.62	0.92	1.76	0.75	0.84	0.84
$3\ ^4\Phi(1)$	$\|\pm2\rangle\|\pm1\rangle$	$0.63(\|1\sigma^2 2\sigma^1 1\pi_x^2 1\pi_y^1 1\delta_-^1\rangle - \|1\sigma^2 2\sigma^1 1\pi_x^1 1\pi_y^2 1\delta_+^1\rangle)$[b]	0.10	0.03	0.04	0.38	0.61	0.61	1.0	1.76	0.74	0.85	0.85
$4\ ^2\Phi(1)$	$\|\pm3\rangle\|0\rangle$	$0.61\|1\sigma^2 2\sigma^1 1\pi_x^2 1\pi_y^1 1\bar{\delta}_-^1\rangle + 0.51\|1\sigma^2 2\sigma^1 1\pi_x^1 1\pi_y^2 1\bar{\delta}_+^1\rangle$[b]	0.10	0.06	0.04	0.37	0.62	0.62	1.0	1.70	0.78	0.84	0.84
$5\ ^4\Delta(1)$	$\|\pm3\rangle\|\mp1\rangle$	$0.77\|1\sigma^2 2\sigma^2 1\pi_x^1 1\pi_y^1 1\delta_-^1\rangle - 0.39\|1\sigma^2 2\sigma^1 \bar{3\sigma}^1 1\pi_x^1 1\pi_y^1 1\delta_-^1\rangle$[c]	0.13	0.05	0.08	1.05	0.21	0.21	1.0	1.83	0.92	0.74	0.74
$6\ ^2\Delta(1)$	$\|\pm3\rangle\|\mp1\rangle$	$0.84\|1\sigma^2 2\sigma^2 1\pi_x^1 1\pi_y^1 1\bar{\delta}_-^1\rangle$[c]	0.11	0.09	0.04	1.0	0.26	0.26	1.0	1.82	0.95	0.72	0.72
$7\ ^2\Pi(2)$	$\|0\rangle\|\pm1\rangle$	$0.44\|1\sigma^2 2\sigma^2 1\pi_x^1 1\pi_y^2\rangle +$ $0.51(\|1\sigma^2 2\sigma^2 1\pi_x^2 1\pi_y^1 1\bar{\delta}_-^1\rangle - \|1\sigma^2 2\sigma^1 1\pi_x^1 1\pi_y^2 1\bar{\delta}_+^1\rangle)$[b]	0.10	0.06	0.05	0.53	0.64	0.71	0.74	1.73	0.86	0.69	0.88
$8\ ^6\Delta(1)$	$\|\pm2\rangle\|0\rangle$	$0.93\|1\sigma^2 2\sigma^1 3\sigma^1 1\pi_x^1 1\pi_y^1 1\delta_-^1\rangle$[c]	0.60	0.02	0.02	0.76	0.25	0.25	1.0	1.79	0.81	0.73	0.73
$9\ ^6\Sigma^+(1)$	$\|\pm1\rangle\|\mp1\rangle$	$0.93\|1\sigma^2 2\sigma^1 1\pi_x^1 1\pi_y^1 1\delta_+^1 1\delta_-^1\rangle$	0.12	0.03	0.02	0.27	0.22	0.22	1.90	1.78	0.82	0.82	0.82
$10\ ^2\Delta(2)$	$\|\pm1\rangle\|\pm1\rangle$	$0.86\|1\sigma^2 1\pi_x^2 1\pi_y^2 1\delta_+^1\rangle$[c]	0.06	0.04	0.06	0.19	0.76	0.76	1.0	1.77	0.16	1.08	1.08
$11\ ^2\Gamma(1)$	$\|\pm3\rangle\|\pm1\rangle$	$0.63\|1\sigma^2 2\sigma^2 1\pi_x^1 \bar{1\pi}_y^1 1\delta_-^1\rangle +$ $0.45(\|1\sigma^2 2\sigma^2 1\pi_x^2 1\delta_+^1\rangle - \|1\sigma^2 2\sigma^2 1\pi_y^2 1\delta_+^1\rangle)$[c]	0.09	0.07	0.04	0.86	0.40	0.40	1.0	1.85	1.10	0.58	0.58
$12\ ^4\Pi(2)$	$\|\pm1\rangle\|0\rangle$	$0.84\|1\sigma^2 2\sigma^1 3\sigma^1 1\pi_x^1 1\pi_y^2\rangle$[b]	0.52	0.03	0.04	0.78	0.45	0.95	0.10	1.75	0.82	0.58	0.95

[a] $|Ti^+;\ a\ ^4F;\ M\rangle|C;\ ^3P;\ M\rangle$. [b] B_1 symmetry component. [c] A_1 symmetry component.

4.2. The TiC^+ Molecule. The TiC^+ results, namely, total energies, dissociation energies, and spectroscopic constants of the 13 examined states, are listed in Table 5, whereas Figure 2 shows the corresponding PECs. Table 6 gives, as in ScC^+, the asymptotic descriptions $|Ti^+>|C>$, dominant CASSCF equilibrium CFs and CASSCF Mulliken atomic distributions, with Figure 3 contrasting relative energy levels of the ScC^+ and TiC^+ molecules.

$X\ ^2\Sigma^+(1)$, $1\ ^2\Pi(1)$. In the ground state and around 5 bohr, an avoided crossing occurs, transferring the equilibrium character of the X state to an M = (0, 0) diabatically correlating state. From the data of Table 6 it seems that the bonding can be represented by scheme (V) of the introduction, amounting to two π bonds and a half σ bond. Note the high population of the $3d_{z^2}$ function (0.61 e^-), suggesting that the in situ metal is in a d^3 configuration, whereas it is in a $4s^13d^2$ configuration at

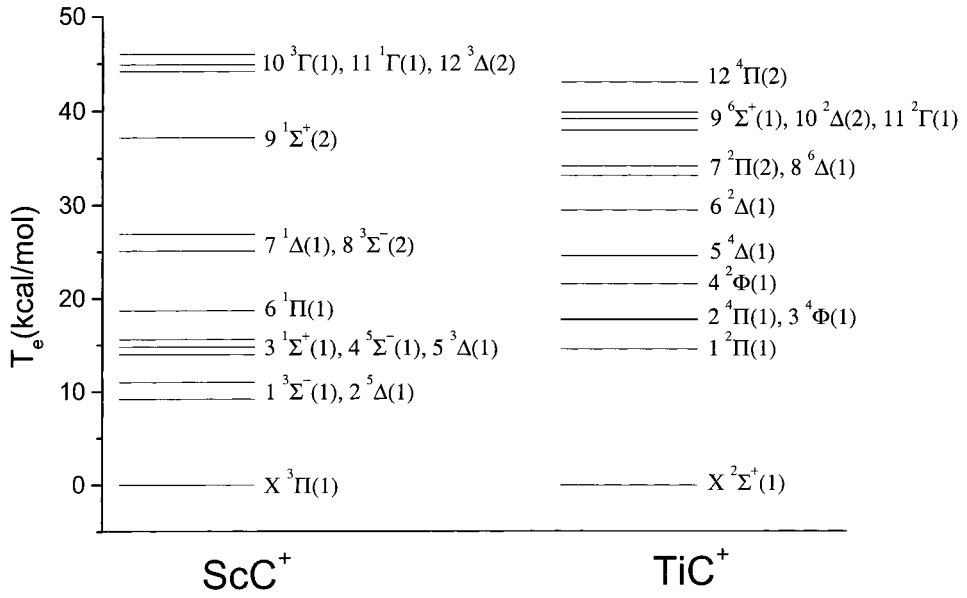

Figure 3. Relative energy levels of the ScC^+ and TiC^+ states studied.

infinity. We surmise that this character change (due to the avoided crossing), is caused by the participation of the Ti^+ a^4P (d^3; M=0) $= \sqrt{4/5}|3d_{z^2}\ 3d_{xz}\ 3d_{yz}\rangle + \sqrt{1/5}|3d_{z^2}\ 3d_{x^2-y^2}\ 3d_{xy}\rangle$ state, 1.17 eV above the ground ^3F state,[5] in complete agreement with the population distribution. While there is no charge transfer via the π skeleton, 0.25 e^- are transferred from Ti^+ to C through the σ frame. At $r_e = 1.696$ Å, a $D_e = 86.4$ (88.0) kcal/mol is predicted at the MRCI (MRCI+Q) level, or $D_0 = D_e - \omega_e/2 =$ 85.2 (86.7) kcal/mol, in fair agreement with the experimental value of 93.4 ± 5.5 kcal/mol (Table 1, ref. 2a).

The first excited state of symmetry 1 $^2\Pi$ lying 14.6 kcal/mol above the X state suffers an avoided crossing at about 4.5 bohr resulting in an interchange of the M quantum number, M = (±1, 0) ← (0, ±1). The bonding (Table 6) is clearly comprised of $1^1/_2$ π bonds and a σ bond; the vbL icon is given in scheme (IV) of the introduction. The bonding situation here is like that of the X $^2\Sigma^+$ state, but with an e^- displacement from the π to the σ frame. At the MRCI level we obtain $D_e = 71.5$ kcal/mol and $r_e = 1.764$ Å, Table 5.

2 $^4\Pi$(1), 3 $^4\Phi$(1). These are two practically degenerate states differing by a mere 0.1 kcal/mol at the MRCI level (or 0.2 kcal/mol at the +Q level); the inclusion of the zero-point energy does not alter the ordering ($|\Delta\omega_e| = 29$ cm^{-1}). Observe the similarity of the CASSCF atomic populations between the two states, Table 6. 3 (= 2 × (0.62 + 0.84)) and 1(= 0.46 + 0.46) e^- are distributed in the π and δ frames, the latter being an "observer" electron. For both states the bonding can be described by the following vbL icon ("+" Π, "−" Φ), suggesting $1^1/_2$ π

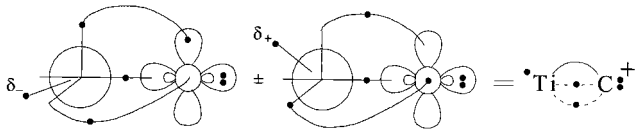

bonds and a half σ bond, with a net transfer of 0.2 e^- from Ti^+ to C. At the MRCI level, the D_es and r_es of the 2 $^4\Pi$ and 3 $^4\Phi$ states are 68.5, 68.4 kcal/mol and 1.853, 1.864 Å, respectively.

4 $^2\Phi$(1), 7 $^2\Pi$(2). At about 4.5 bohr the 4 $^2\Phi$ state experiences an avoided crossing with another (unidentified) $^2\Phi$ state. The asymptotic CASSCF populations ($4s^{1.0}\ 3d_{xz}^{0.5}\ 3d_{yz}^{0.5}\ 3d_{x^2-y^2}^{0.5}\ 3d_{xy}^{0.5}/2s^{1.95}\ 2p_z^{0.05}\ 2p_x^{1.0}\ 2p_y^{1.0}$) in conjunction with the corresponding equilibrium populations and dominant configurations (Table 6, B_1 component), lead to a bonding picture with a 1 1/2 π and a half σ bond,

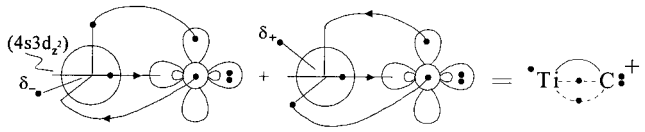

Through the π frame 0.3 e^- are transferred from C to Ti^+, while 0.5 e^- return to the C atom via the σ frame. With respect to $Ti^+(a^4F)$ + C(^{3}P), $D_e = 64.9$ kcal/mol at $r_e = 1.899$ Å at the MRCI level.

Two of the leading CFs of the 7 $^2\Pi$ state are the same with those of the 4 $^2\Phi$ state, with the third one being the same as that of the 1 $^2\Pi$ state (Table 6). Not much can be said about the bonding of this state. Again a total transfer of 0.2 e^- is recorded from Ti^+ to the C atom, with a $D_e = 53.5$ kcal/mol and $r_e = 1.860$ Å.

5 $^4\Delta$(1), 6 $^2\Delta$(1), 10 $^2\Delta$(2). As can be seen from Table 6, the only difference between the fifth and the sixth states is the spin multiplicity. The asymptotic CASSCF Mulliken distributions ($4s^{1.0}\ 3d_{xz}^{0.5}\ 3d_{yz}^{0.5}\ 3d_{x^2-y^2}^{0.5}\ 3d_{xy}^{0.5}/2s^{1.96}\ 2p_z^{1.0}\ 2p_x^{0.52}\ 2p_y^{0.52}$) coupled with the data of Table 6 indicate, for both the 5th and the 6th states, the following bonding scenario (A_1 component):

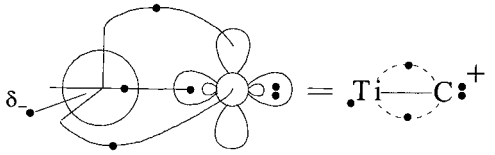

or two-half π bonds and a single σ bond (in the A_2 component the $3d_{xy}$ (δ_-) e^- is hosted by a $3d_{x^2-y^2}$ (δ_+) orbital). In essence, a spin flip of the $3d_{xy}$ (or $3d_{x^2-y^2}$) e^- leads from the 5 $^4\Delta$ to the 6 $^2\Delta$ state. The Ti^+ cation loses 0.45 e^- through the π system, gaining at the same time ~0.2 e^- through the σ frame. At the MRCI level, the dissociation energies and bond distances are $D_e = 61.8$, 56.9 kcal/mol and $r_e = 1.911$, 1.945 Å, for 5 $^4\Delta$ and 6 $^2\Delta$ states, respectively.

It is of interest to mention that the 6 $^2\Delta$ state experiences an avoided crossing around 3.30 bohr, i.e., on the repulsive part of its PEC, with the 10 $^2\Delta$ state. The dominant configuration and the Mulliken populations dictate a triple bond, exactly as in the 3 $^1\Sigma^+$ state of ScC^+, scheme (III) of the introduction. Notice the striking similarities between the populations of the 10 $^2\Delta$ and 3 $^1\Sigma^+$ states of TiC^+ and ScC^+, respectively (Tables 4 and 6); the symmetry-carrying electron of the 10 $^2\Delta$ state (δ_+ in A_1 component) does not participate in the bonding, being completely localized on the metal. At $r_e = 1.803$ Å, the $D_e =$ 47.5 kcal/mol with respect to $Ti^+(a^4F) + C(^3P)$.

8 $^6\Delta$*(1),* *9* $^6\Sigma^+$*(1).* Due to high spin, the chemistry of both is captured within a single reference (Hartree−Fock) description, Table 6. The equilibrium Mulliken distributions, for both states, clearly dictate $^3/_2$ bonds, two half-π, and one half-σ; in the A_1 component, the binding icon for the $^6\Delta$ state is

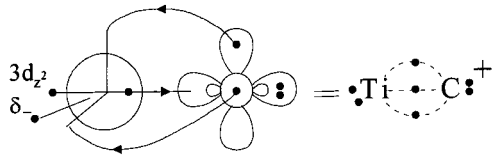

Approximately 0.5 e^- are moving through the π system from C to Ti^+, while 0.6 e^- from Ti^+ to C through the σ frame. From the $^6\Delta$ state, the $^6\Sigma^+$ state is obtained by repositioning the $3d_\sigma$ ($3d_{z^2}$) e^- to a δ_+ orbital:

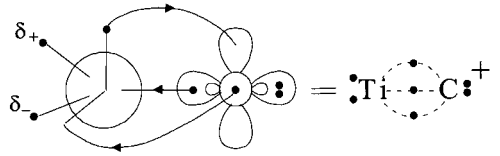

Overall, 0.25 e^- are transferred from Ti^+ to the C atom. Notice the equality of bond lengths between the two states and a difference of 3.5 kcal/mol in their D_e values, Table 5.

11 $^2\Gamma$*(1).* Some technical difficulties prevented us from calculating a complete PEC, i.e., starting from infinity we were forced to stop at 3.6 bohr, with $r_e = 3.7$ bohr. Comparing the asymptotic CASSCF distributions

$$(4s^{1.0}\ 3d_{xz}^{0.5}\ 3d_{yz}^{0.5}\ 3d_{x^2-y^2}^{0.5}\ 3d_{xy}^{0.5}/2s^{1.96}\ 2p_z^{1.0}\ 2p_x^{0.52}\ 2p_y^{0.52})$$

with the corresponding ones at r_e, no drastic changes are observed, apart from the usual transfer of the 4s e^- to the $3d_{z^2}$ orbital. Taking also into account the dominant configurations, the following bonding icon can be given (A_1 symmetry)

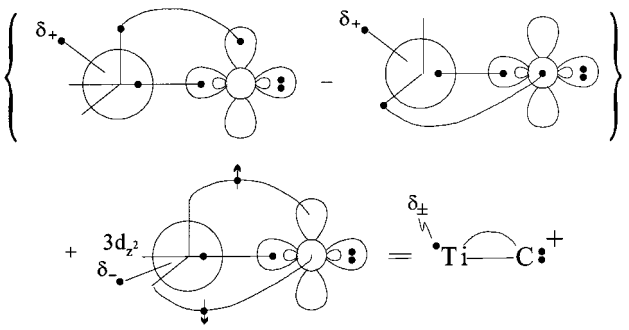

12 $^4\Pi$*(2).* This is the last state discussed in the present report, located 43 kcal/mol above the X state. The irregularity shown in the PEC around 4.5 bohr (Figure 2) could be caused by its interaction with the previously discussed 2 $^4\Pi(1)$ state. At the same point, abrupt changes are observed in the population distributions as compared with the asymptotic ones

$$(4s^{1.0}\ 3d_{z^2}^{0.40} 3d_{xz}^{0.50}\ 3d_{yz}^{0.50}\ 3d_{x^2-y^2}^{0.30}\ 3d_{xy}^{0.30}/2s^{1.96}\ 2p_z^{0.04}\ 2p_x^{1.0}\ 2p_y^{1.0})$$

$$\delta_\pm^{0.60}(r_\infty) \rightarrow \delta_\pm^{1.0}(r = 4.5\ \text{bohr}) \rightarrow \delta_\pm^{0.10}(r_e)$$

$$d_\pi^{1.0}(r_\infty) \rightarrow d_\pi^{0.20}(r = 4.5\ \text{bohr}) \rightarrow d_\pi^{1.40}(r_e)$$

$$d_\sigma^{0.40}(r_\infty) \rightarrow d_\sigma^{0.96}(r = 4.5\ \text{bohr}) \rightarrow d_\sigma^{0.78}(r_e)$$

At equilibrium we can discern the formation of $1^1/_2$ π bonds and one half σ bond, with a total transfer of 0.13 e^- from Ti^+ to C. The predicted D_e and r_e are 43.7 kcal/mol and 1.875 Å at the MRCI level.

TABLE 7: Comparison of D_e (kcal/mol), r_e (Å), ω_e (cm^{-1}), and Mulliken Charges on the Metal, q_M, of the Ground States of the Two Series ScZ^+ and TiZ^+, Z = B, C, N and O (experimental D_0 values in parentheses)

species and binding mode	state	D_e	r_e	ω_e	q_M
Sc–B^{+a}	X $^4\Sigma^-$	44.9	2.160	513	+1.08
Sc–C^{+b}	X $^3\Pi$	69.8 (77.0)[c]	1.908	709	+1.30
Sc–N^{+d}	X $^2\Sigma^+$	84.2	1.738	871	+1.49
Sc–O^{+e}	X $^1\Sigma^+$	146.0 (164.6)[f]	1.651	1134	+1.28
Ti–B^{+g}	X $^5\Delta$	47.6	2.102	519	+1.0
Ti–C^{+b}	X $^2\Sigma^+$	86.4 (93.4)[c]	1.696	859	+1.23
Ti–N^{+d}	X $^1\Sigma^+$	110.7 (119.7)[h]	1.586	1045	+1.43
Ti–O^{+i}	$^2\Delta$ (?)[i]	(158.6)[f]			

[a] Reference 14. [b] Present work. [c] Reference 2a. [d] References 1 and 17; see also ref 18. [e] References 1 and 19. [f] Reference 20. [g] Reference 11. [h] Reference 21. [i] Assumed by the present authors; the single e^- on Ti is of $\delta_\pm$ symmetry and the in situ Ti atom is assumed to be in its b^4F state.

5. Synopsis and Remarks

With the purpose of obtaining reliable structural parameters and bonding insights, we have investigated the diatomic carbide cations ScC^+ and TiC^+ via multireference CI valence techniques (CASSCF+1+2) coupled with quantitative basis sets. We report total energies, r_e, D_e, ω_e, $\omega_e x_e$, T_e and potential energy curves for 13 ScC^+ and 13 TiC^+ states. As far as we know these are the first theoretical results on these molecular ions to be reported in the literature. Our main findings are summarized as follows.

All 26 states are bound with respect to the ground-state atoms, $Sc^+(^3D)$, $Ti^+(a^4F) + C(^3P)$, with binding energies ranging from 86.4 kcal/mol, X $^2\Sigma^+$ (TiC^+), to 23.8 kcal/mol, 12 $^3\Delta(2)$ (ScC^+). Figure 3 compares the relative energy levels of both ScC^+ and TiC^+ species. Note that certain states are degenerate within the

accuracy of our methods; extreme cases are the 2 $^4\Pi(1)$ and 3 $^4\Phi(1)$ states of TiC^+, with ΔT_e (ΔT_0) = 0.1 (0.1) kcal/mol.

The ground states of ScC^+ and TiC^+ are of $^3\Pi$ and $^2\Sigma^+$ symmetries, with binding energies of 69.8 (72.5) and 86.4 (88.0) kcal/mol, respectively, at the MRCI (MRCI+Q) level of theory. These numbers compare favorably with the existing experimental D_0 values of 77.0 ± 1.4 kcal/mol (ScC^+) and 93.4 ± 5.5 kcal/mol (TiC^+). It is interesting to contrast the binding modes and certain characteristic quantities of the series ScZ^+ and TiZ^+, where Z = B, C, N, and O, Table 7.

For both series, note the monotonic increase in the D_e and ω_e values, with a corresponding decrease in bond lengths, as a function of the number of bonding electrons. Also, everything is in line with the charge transfer from M^+ to Z: the e^- transfer increases moving from B to N, and then decreases (ScO^+) as expected due to the strong donating character of the $2p_\sigma$ oxygen electrons. We are entitled to assume that the same thing holds for the TiO^+ case. Observe as well the preference of filling the π system rather than the σ bonding skeleton, as we move from B to O.

Finally, it should be mentioned that in all states studied, a negative charge transfer of about 0.2−0.3 e^- is recorded from the metal cation to the carbon atom. More or less, the same is observed for the borides and nitrides, and could be rationalized by remembering the rather low ionization potential (IP) of the first-row transition metal cations (for instance less than the IP of the hydrogen atom in the Sc^+ case), and the Coulombic stabilization that is caused by this kind − and not the opposite− electron transfer.

Acknowledgment. The financial support of the National and Kapodistrian University of Athens through its Special Research Account for Basic Research is greatly appreciated. I.S.K.K. thanks the Hellenic State Scholarships Foundation (I.K.Y.) for financial assistance.

References and Notes

(1) See for instance, Harrison, J. F. *Chem. Rev.* **2000**, *100*, 679, and references therein.

(2) (a) Clemmer, D. E.; Elkind, J. L.; Aristov, N.; Armentrout, P. B. *J. Chem. Phys.* **1991**, *95*, 3387. (b) Aristov, N.; Armentrout, P. B. *J. Am. Chem. Soc.* **1986**, *108*, 1806.

(3) Hettich, R. L.; Freiser, B. S. *J. Am. Chem. Soc.* **1986**, *108*, 2537.

(4) Harrison, J. F. *J. Phys. Chem.* **1986**, *90*, 3313.

(5) Moore, C. E. *Atomic Energy Levels*; NSRDS−NBS Circular No. 35; U. S. GPO: Washington, DC, 1971.

(6) Bauschlicher, C. W., Jr. *Theor. Chim. Acta* **1995**, *92*, 183.

(7) Dunning, T. H., Jr. *J. Chem. Phys.* **1989**, *90*, 1007.

(8) Werner, H.-J.; Knowles, P. J. *J. Chem. Phys.* **1988**, *89*, 5203. Knowles, P. J.; Werner, H.-J.; Reinsch, E. A. *J. Chem. Phys.* **1982**, *76*, 3144. Werner, H.-J. *Adv. Chem. Phys.* **1987**, *LXIX*, 1.

(9) Docken, K.; Hinze, J. *J. Chem. Phys.* **1972**, *57*, 4928.

(10) Werner, H.-J.; Meyer, W. *J. Chem. Phys.* **1981**, *74*, 5794.

(11) Kalemos, A.; Mavridis, A. *J. Phys. Chem. A* **1998**, *102*, 5982.

(12) Boys, S. F.; Bernardi, F. *Mol. Phys.* **1970**, *19*, 553.

(13) MOLPRO is a package of ab initio programs written by, H.-J. Werner and P. J. Knowles, with contributions from J. Almlöf, R. D. Amos, A. Berning, M. J. O. Deegan, F. Eckert, S. T. Elbert, C. Hampel, R. Lindh, W. Meyer, A. Nicklass, K. Peterson, R. Pitzer, A. J. Stone, P. R. Taylor, M. E. Mura, P. Pulay, M. Schuetz, H. Stoll, T. Thorsteinsson, and D. L. Cooper.

(14) Kalemos, A.; Mavridis, A. *Adv. Quantum Chem.* **1998**, *32*, 69.

(15) Bunge, C. F.; Barrientos, J. A.; Bunge, A. V.; Cogordan, J. A. *Phys. Rev. A* **1992**, *46*, 3691.

(16) (a) Langhoff, S. R.; Davidson, E. R. *Int. J. Quantum Chem.* **1974**, *8*, 61. (b) Blomberg, M. R. A.; Siegbahn, P. E. M. *J. Chem. Phys.* **1983**, *78*, 5682.

(17) Kunze, K. L.; Harrison, J. F. *J. Phys. Chem.* **1989**, *93*, 2983.

(18) Elkhattabi, S.; Daoudi, A.; Flament, J. P.; Berthier, G. *Chem. Phys.* **1999**, *241*, 257.

(19) Tilson, J. L.; Harrison, J. F. *J. Phys. Chem.* **1991**, *95*, 5097.

(20) Armentrout, P. B.; Kickel, B. L. *Organometallic Ion Chemistry*; Freiser, B., Ed.; Kluwer Academic Publishers: Dodrecht, 1996; pp 1−45.

(21) Clemmer, D. E.; Sunderlin, L. S.; Armentrout, P. B. *J. Phys. Chem.* **1990**, *94*, 3008.